

A study on methanol steam reforming to CO₂ and H₂ over the La₂CuO₄ nanofiber catalyst

Lizhen Gao^{a,*}, Gebiao Sun^b, Sibudjing Kawi^b

^aSchool of Mechanical Engineering M050, The University of Western Australia, 35 Stirling Highway, Crawley, WA 6009, Australia

^bDepartment of Chemical and Biomolecular Engineering, National University of Singapore, 4 Engineering Drive 4, Singapore 117576, Republic of Singapore

Received 6 July 2007; received in revised form 15 October 2007; accepted 30 October 2007

Available online 5 November 2007

Abstract

The La₂CuO₄ crystal nanofibers were prepared by using single-walled carbon nanotubes as templates under mild hydrothermal conditions. The steam reforming of methanol (SRM) to CO₂ and H₂ over such nanofiber catalysts was studied. At the low temperature of 150 °C and steam/methanol = 1.3, methanol was completely (100%, 13.8 g/h g catalyst) converted to hydrogen and CO₂ without the generation of CO. Within the 60 h catalyst lifespan test, methanol conversion was maintained at 98.6% (13.6 g/h g catalyst) and with 100% CO₂ selectivity. In the meantime, for distinguishing the advantage of nanoscale catalyst, the La₂CuO₄ bulk powder was prepared and tested for the SRM reaction for comparison. Compared with the La₂CuO₄ nanofiber, the bulk powder La₂CuO₄ showed worse catalytic activity for the SRM reaction. The 100% conversion of methanol was achieved at the temperature of 400 °C, with the products being H₂ and CO₂ together with CO. The catalytic activity in terms of methanol conversion dropped to 88.7% (12.2 g/h g catalyst) in 60 h. The reduction temperature for nanofiber La₂CuO₄ was much lower than that for the La₂CuO₄ bulk powder. The nanofibers were of higher specific surface area (105.0 m²/g), metal copper area and copper dispersion. The *in situ* FTIR and EPR experiments were employed to study the catalysts and catalytic process. In the nanofiber catalyst, there were oxygen vacancies. H₂-reduction resulted in the generation of trapped electrons [e] on the vacancy sites. Over the nanofiber catalyst, the intermediate H₂CO/HCO was stable and was reformed to CO₂ and H₂ by steam rather than being decomposed directly to CO and H₂. Over the bulk counterpart, apart from the direct decomposition of H₂CO/HCO to CO and H₂, the intermediate H₂COO might go through two decomposition ways: H₂COO = CO + H₂O and H₂COO = CO₂ + H₂.

© 2007 Elsevier Inc. All rights reserved.

Keywords: La₂CuO₄ nanofiber; Methanol steam reforming; CO₂ selectivity; *In situ* FTIR

1. Introduction

Hydrogen has been envisaged to be the ideal clean energy in the future [1,2]. The difficulty in wide usage of hydrogen is its storage and distribution [3,4]. Before a highly effective hydrogen storage material (more than 6.5 wt% hydrogen can be stored and released under a mild condition) is discovered, the on-board generation of hydrogen from liquid fuel such as methanol with high energy density will be an option [5,6]. Through three ways methanol can be transformed to hydrogen, i.e. (i) the direct decomposition of methanol (CH₃OH = CO + 2H₂);

(ii) partial oxidation of methanol (CH₃OH + 1/2O₂ = CO₂ (or CO) + 2H₂) and (iii) steam reforming of methanol (SRM) (CH₃OH + H₂O = CO₂ + 3H₂) [7]. Amongst the three ways, (i) and (ii) will produce a considerable amount of CO as a product or by-product. In the hydrogen fuel cell, even a trace of CO can deteriorate the Pt electrode [5,6,8]. The SRM process produces H₂ and CO₂ with the molar ratio of 3/1 (the highest amongst the three ways) as well as a little CO as a by-product [7], so it has been regarded as the most suitable on-board process to generate hydrogen. So far the most extensively studied catalysts for SRM are Cu/ZnO/Al₂O₃ [9,10], Cu/ZrO₂ [11], Al–Cu–Fe [12], etc., which are also the methanol synthesis catalysts from syngas. The problems we have to overcome are (i) the high reaction temperature to obtain the high conversion of

*Corresponding author. Fax: +61 8 64881024.

E-mail address: lizhen@mech.uwa.edu.au (L. Gao).

methanol. Even over the most effective catalyst, 100% methanol conversion can only be achieved at temperatures above 300 °C [7,13]; (ii) the formation of CO at the high conversion of methanol at high temperatures. Apart from the Cu–Zn–Al series catalysts, the perovskite-structured complex cuprites (such as $\text{YBa}_2\text{Cu}_3\text{O}_7$) have been demonstrated to be good catalysts for methanol synthesis from syngas [14]. Recently we have successfully synthesized perovskite-like La_2CuO_4 single-crystal nanofibers (ca. 30 nm in diameter and 3 μm in length) by using single-walled carbon nanotubes (SWNTs; ca. 2 nm in inner diameter; made *via* CH_4 cracking over the catalyst of $\text{Mg}_{0.8}\text{Mo}_{0.05}\text{Ni}_{0.10}\text{Co}_{0.05}\text{O}_x$ at 800 °C) as templates under mild hydrothermal conditions and a temperature around 60 °C [15]. Here we report our results that such La_2CuO_4 nanofibers showed an excellent catalytic performance for SRM reaction. The 100% methanol conversion could be reached at the low temperature of 150 °C. There was no significant drop in activity within 60 h reaction test on stream. No CO was created below the temperature of 300 °C. To distinguish the advantage of the nanofiber state of the catalyst, the La_2CuO_4 bulk powder counterpart was prepared and tested for comparison as well. Techniques such as TGA, *in situ* FTIR (diffuse reflectance infrared Fourier transform spectroscopy—DRIFT) and EPR were employed to study the catalysts and the SRM mechanism.

2. Experimental section

Detailed descriptions about the synthesis of SWNTs and La_2CuO_4 nanofibers by using SWNTs as templates were described in our previous publication [15]. Briefly, the SWNTs were home-made by cracking of CH_4 ($\text{CH}_4/\text{H}_2/\text{He} = 1/1/8$) at 800 °C over a mixed-oxide catalyst $\text{Mg}_{0.8}\text{Mo}_{0.05}\text{Ni}_{0.10}\text{Co}_{0.05}\text{O}_x$. The SWNT sample was purified by nitric-acid washing repeatedly in an ultrasonic bath. The carbon nanotubes (CNTs) were single walled with a 2 nm in-average inner diameter. For hydrothermal synthesis of La_2CuO_4 single-crystal nanofibers by using SWNTs as templates, the mixed solution of the surfactant poly(ethylene glycol)-block-poly(propylene glycol)-block-poly(ethylene glycol), $\text{La}(\text{NO}_3)_3 \cdot 6\text{H}_2\text{O}$ and $\text{Cu}(\text{NO}_3)_2 \cdot 6\text{H}_2\text{O}$ (according to the stoichiometric composition of La_2CuO_4), SWNTs and H_2O_2 was dispersed ultrasonically and was put into an autoclave for hydrothermal synthesis at 60 °C for 20 h. The precipitation obtained from hydrothermal synthesis was filtered and washed with distilled water repeatedly and then was heated at 110 °C for 1 h. Thus the La_2CuO_4 nanofibers were synthesized. The La_2CuO_4 bulk powder catalyst was prepared by heating the solution of $\text{La}(\text{NO}_3)_3 \cdot 6\text{H}_2\text{O}$, $\text{Cu}(\text{NO}_3)_2 \cdot 6\text{H}_2\text{O}$ (molar ratio of $\text{La}/\text{Cu} = 2/1$) and citric acid at 50 °C until a syrup was formed, followed by heating in air at 700 °C for 6 h.

To remove the CNTs in La_2CuO_4 , the sample was put into a quartz tube positioned in a tubular furnace. The air flow (flow rate: 30 ml/min) was conducted into the tube and

the sample was heated (heating rate: 5°/min) to 700 °C and kept at 700 °C for 2 h. The effluent was monitored by GC. The CNT oxidation caused CO_2 formation. When we could not observe CO_2 formation, we believed that the CNTs have been completely oxidized.

The SRM reaction was carried out on a fixed bed flow reactor at atmospheric pressure by using 100 mg of catalyst. The catalyst was reduced at 500 °C for 1 h in the flow of H_2/N_2 (5/95, v/v; flow rate = 35 ml/min) prior to SRM reaction. The feed gas composition was $\text{MeOH}/\text{H}_2\text{O} = 1/1.3$ (molar ratio). Flow rate of reagent was 0.04 ml/min (liquid). The products were analyzed online by GC.

The contents of copper in different oxidation states were estimated by means of iodometry according to the procedures adopted by Harris and Hewston [16]. The oxygen non-stoichiometry values were calculated from the amount of Cu^{2+} , Cu^+ or Cu^{3+} present, assuming that the La^{3+} was in its stable oxidation state [17]. The copper surface area and dispersion were measured using a nitrous oxide titration [18]. Prior to N_2O surface titration, samples were reduced in a 5% H_2/He stream at 500 °C, followed by cooling to 150 °C under a flow of helium. A known volume of N_2O was then injected in pulses by using a 6-port valve, and the N_2 and N_2O in the effluent were analyzed by a GC–MS system. The copper metallic surface area and dispersion were calculated by assuming 1.46×10^{19} copper atoms/ m^2 and a molar stoichiometry $\text{N}_2\text{O}/\text{Cu}_s = 0.5$, where Cu_s implies the copper atom on the surface.

The morphologies of La_2CuO_4 nanofibers and bulk powder were observed under a transmission electron microscope (JEOL, JEM 2010) and a field emission scanning electron microscope (FESEM) (JEOL, JSM 7600F). The thermogravimetric (TG) curves in hydrogen atmosphere were obtained on a Shimadzu DTG-60 thermal analysis instrument.

EPR spectra were recorded at -196 °C with a JEOL spectrometer operating in the *x*-band and calibrated with a DPPH standard ($g = 2.004$). About 0.2 g of catalyst was placed in a self-made quartz cell in which the sample could be treated under different atmospheres at various temperatures. Before performing the EPR studies over the samples, the sample was He-purged (flow rate, 20 ml/min) at 25 °C for 1 h; then H_2 ($\text{H}_2/\text{He} = 5/95$, total flow rate = 30 ml/min) was introduced into the quartz cell at 500 °C for 1 h, followed by He-purging at the same temperature and quenching (-196 °C) for EPR analysis.

In situ FTIR spectra (DRIFT) were collected on a Nicolet series II magna-IR 550 spectrometer with a SPECTRA TECH *in situ* cell. The catalyst powder weighing approximately 50 mg was contained in a low-dead volume infrared cell. The cell was heated by means of an electrical resistance heater. Before FTIR spectrum collection, the cell was pumped for 10 min to remove gaseous CO_2 and H_2 . *In situ* absorbance spectra were obtained at 4 cm^{-1} resolution. Methanol was injected into the cell at the temperature of 350 °C. The spectra were then

referenced to a spectrum of the catalyst collected at the same temperature under a H_2 flow ($H_2/N_2 = 5/95$, v/v, 20 ml/min.).

Pulse reaction was carried out on a pulse microreactor system. Each pulse volume was 67.5 μ l. During the reaction, He was used as the carrier gas (flow rate, 20 ml/min). The products were checked by a GC–MS system.

The BET specific surface area of the catalysts was determined by nitrogen adsorption data at $-196^\circ C$ on a Nova 1200 system.

3. Results and discussion

The FESEM images of as-synthesized La_2CuO_4 nanofibers are shown in Fig. 1A in which we observe groups of aligned microfibers. The length of the fiber is close to 3 μ m. Fig. 1B is the enlarged FESEM image for the individual fibers. The average diameter of the fibers is around 60 nm. XRD result has confirmed that these single-crystal fibers are of La_2CuO_4 crystal structure [15]. We are not sure whether or not there are SWNTs inside the La_2CuO_4 nanofibers. So we have treated the as-synthesized La_2CuO_4 nanofibers in air at $700^\circ C$ for 2 h for further purification before catalytic activity measurement. At $700^\circ C$ in air, the CNTs would be burnt out completely as we cannot observe any more CO_2 formation. We have found that the CNTs

could be completely oxidized to CO_2 at temperatures around $650^\circ C$ [19,20].

The FESEM image of the $700^\circ C$ -treated nanofibers is shown in Fig. 1C. The diameter of La_2CuO_4 nanofibers is around 30 nm. We deduce that the shrinkage of La_2CuO_4 nanofibers is due to the combustion of SWNTs inside it.

Table 1 shows the composition, BET specific surface area, Cu metal area and dispersion of the La_2CuO_4 nanofiber and bulk powder. In the La_2CuO_4 bulk powder, there are Cu^{3+} and Cu^{2+} while in the nanofibers there are Cu^{2+} and Cu^+ . In the bulk powder sample, the oxygen is over-stoichiometric, while in the nanofiber counterpart, there are the oxygen vacancies. The BET specific surface areas of La_2CuO_4 nanofibers (treated at $700^\circ C$ in air) and

Table 1
Composition, BET specific surface area, Cu-metal area, Cu dispersion of La_2CuO_4 nanofiber and bulk powder

Catalyst	Composition	BET surface area (m^2/g)	Cu-metal area (m^2/g)	Cu dispersion (%)
Nanofibers	$La_2Cu_{0.88}^{2+}Cu_{0.12}^{+}O_{3.94}$	105.0	10.8	40.21
Bulk powder	$La_2Cu_{0.92}^{2+}Cu_{0.08}^{3+}O_{4.04}$	2.7	1.5	5.78

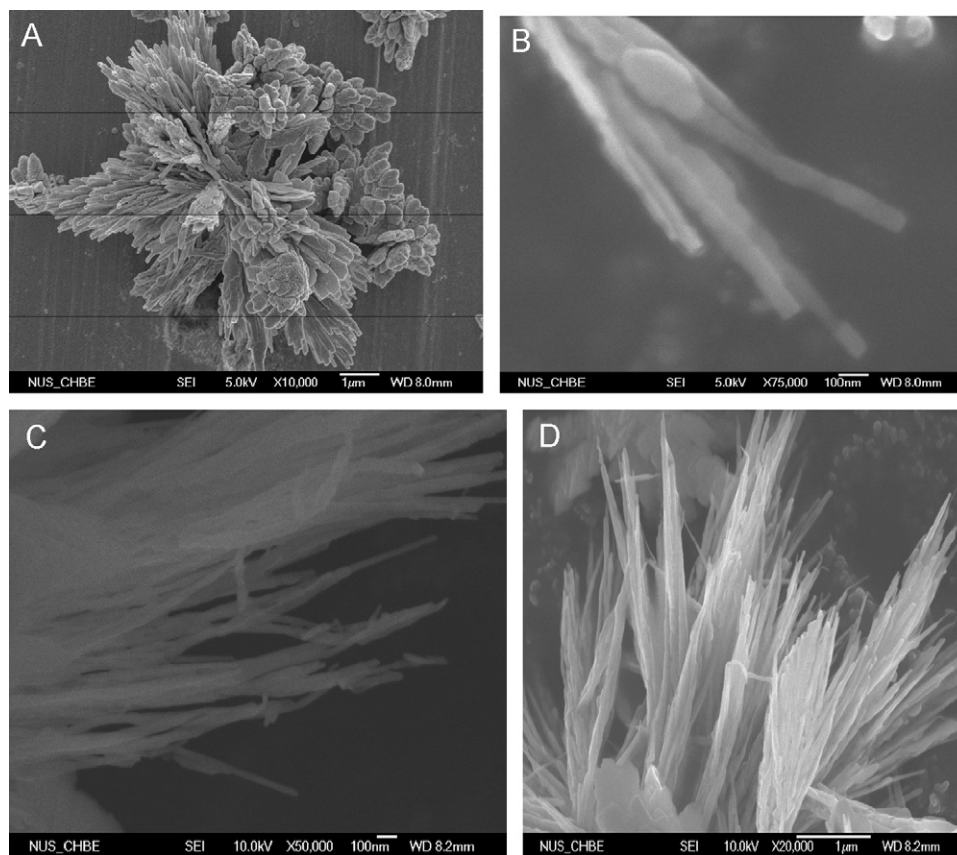


Fig. 1. FESEM images of La_2CuO_4 single-crystal nanofibers (hydrothermal synthesis for 20 h). (A) Groups of highly oriented and uniform-diameter fibers; (B) an enlarged image of some individual fibers; (C) after being treated in air at $700^\circ C$ for 1 h; (D) after being tested for SRM reaction lifespan for 60 h.

Table 2
Activity and selectivity for steam reforming of methanol over nanofiber La_2CuO_4 and bulk powder La_2CuO_4

Catalyst	Reaction temperature ($^{\circ}\text{C}$)	Conv. of MeOH (%)	Conv. of MeOH (g/h g catalyst)	Selectivity (%)		Rate of H_2 production (g/h g catalyst)
				CO_2	CO	
La_2CuO_4 nanofibers	100	52.4	7.23	100.00	0	1.11
	150	100.0	13.8	100.00	0	2.11
	200	100.0	13.8	100.00	0	2.11
	250	100.0	13.8	100.00	0	2.11
	300	100.0	13.8	100.00	0	2.11
	350	100.0	13.8	99.98	0.02	2.09
	400	100.0	13.8	99.95	0.05	2.05
Bulk powder La_2CuO_4	200	6.7	0.92	98.64	1.36	0.13
	250	11.2	1.55	98.02	1.98	0.23
	300	16.4	2.26	97.45	2.55	0.34
	350	51.7	7.13	97.00	3.00	1.06
	400	100.0	13.8	96.52	3.45	2.03

bulk powder are 105.0 and 2.7 m^2/g , respectively. So far the highest specific area reported for La_2CuO_4 catalyst is 13.0 m^2/g prepared by sol–gel method [21]. The copper metal area and dispersion over the nanofibers are both much higher than those over the bulk powder. The higher dispersion of copper metal is beneficial for the methanol steam reforming reaction.

The catalytic activities of the La_2CuO_4 nanofiber and bulk powder catalysts for the SRM reaction are summarized in Table 2. Over the nanofiber catalyst, at 100 $^{\circ}\text{C}$, the methanol conversion is 52.4% (7.23 g/h g catalyst). When the temperature is elevated to 150 $^{\circ}\text{C}$, 100% methanol is converted (13.8 g/h g catalyst). At temperatures below 300 $^{\circ}\text{C}$, the products are only H_2 and CO_2 without CO. In SRM reaction, CO is generated by the reverse water–gas-shift reaction: $\text{CO}_2 + \text{H}_2 = \text{CO} + \text{H}_2\text{O}$. This means that the nanofiber catalyst can suppress this reaction. When the reaction temperatures are at 350 and 400 $^{\circ}\text{C}$, only 0.02% CO ($\text{CO}_2/\text{CO} = 99.98/0.02$) and 0.05% CO ($\text{CO}_2/\text{CO} = 99.95/0.05$) are detected, respectively. Over the bulk powder La_2CuO_4 catalyst, below 200 $^{\circ}\text{C}$, little methanol has been reformed to hydrogen and either CO or CO_2 . At temperatures of 200, 250, 300 and 350 $^{\circ}\text{C}$, the methanol conversion is 6.7% (0.92 g/h g catalyst), 11.2% (1.55 g/h g catalyst), 16.4% (2.26 g/h g catalyst) and 51.7% (7.13 g/h g catalyst), respectively. At the temperature of 400 $^{\circ}\text{C}$, 100% methanol (13.8 g/h g catalyst) can be reformed. In all the tested temperatures, the products are H_2 , CO_2 and CO. The CO selectivity is positively dependent on the temperatures (200 $^{\circ}\text{C}$: 1.36%; 400 $^{\circ}\text{C}$: 3.45%). Obviously the catalytic activity over nanofiber La_2CuO_4 catalyst is much better than that over its powder counterpart. CO concentration increased with the rise of temperature [22].

The lifetimes of both the nanofiber (at 250 $^{\circ}\text{C}$) and the bulk powder (at 400 $^{\circ}\text{C}$) catalysts are tested within 60 h and the results are shown in Fig. 2. Over the nanofiber catalyst, in the beginning 23 h, no activity drop can be observed and afterwards the methanol conversion slightly decreases and

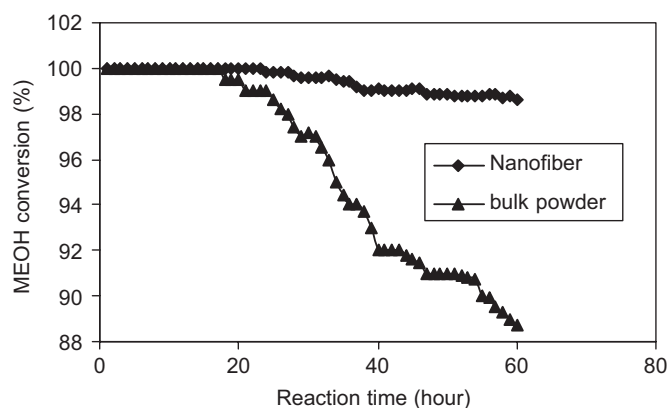


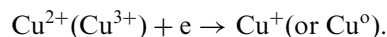
Fig. 2. Methanol conversions as a function of time-on-stream over (\blacklozenge) nanofiber La_2CuO_4 catalyst at 250 $^{\circ}\text{C}$ and (\blacktriangle) bulk powder La_2CuO_4 catalyst at 400 $^{\circ}\text{C}$.

finally drops down to 98.6% (13.6 g/h g catalyst) in the 60th hour without CO formation. The CO_2 selectivity is still 100%. Over the powder catalyst, in the beginning 17 h, there is no activity drop, while in the following 43 h, the activity declines to 88.7% (12.2 g/h g catalyst) of methanol conversion with the CO selectivity of 4.2%. So in terms of the lifespan, the nanofiber catalyst is also superior to the bulk powder. With respect to the fact that the lifetime test for the nanofibers is conducted at lower (250 $^{\circ}\text{C}$) temperature than that (400 $^{\circ}\text{C}$) for the bulk powder, we have also examined the methanol conversion of La_2CuO_4 nanofibers at 400 $^{\circ}\text{C}$ for 60 h and found that even at such conditions, the methanol conversion was maintained at 98.0% (13.5 g/h g catalyst). Even using the Pd-based methanol-reforming catalysts and microstructured reactors, 85% methanol conversion was achieved at 310 $^{\circ}\text{C}$ (steam/ethanol = 1.9); CO concentration was 0.2–0.5% [23]. Over the advanced plate-fin reformer, the device incorporates methanol steam reforming ($\text{Cu}/\text{Zn}/\text{Al}_2\text{O}_3$) with catalytic combustion ($\text{Pt}/\text{Al}_2\text{O}_3$); 100% methanol

conversion was obtained over 100 h at temperatures of 210–270 °C (steam/methanol = 1.2–1.6). But the CO concentration steadily increased over this time from 0.4% to 1.2% [24].

Fig. 1D is the FESEM image of a La_2CuO_4 nanofiber after being tested for catalytic activity lifespan for 60 h. No significant sintering is observed from Fig. 1D, indicating that the nanofiber catalyst is still quite fresh. The BET specific surface area of the lifespan-tested nanofiber is $97.3 \text{ m}^2/\text{g}$, a little decrease in comparison with the original value of $105 \text{ m}^2/\text{g}$, while the specific surface area of the lifespan-tested La_2CuO_4 bulk powder is only $0.9 \text{ m}^2/\text{g}$. The biggest problem with the Cu-based catalyst is the tendency for copper crystallites to readily sinter at the temperatures $> 300 \text{ }^\circ\text{C}$ [25]. On the other hand, the coke generated by the side reactions of SRM may deactivate the powder catalyst. The energy-dispersive X-ray analysis reveals that there is a carbon element on the surface of the used powder catalyst.

Both the methanol synthesis reaction and the SRM reaction over cupric catalysts follow a redox mechanism [14,26]. Therefore we studied the reducibility of the La_2CuO_4 nanofiber and powder. The TG curves of La_2CuO_4 nanofiber and bulk powder in hydrogen atmosphere are shown in Fig. 3A and B. Both the nanofiber and powder La_2CuO_4 catalysts show one weight-loss step. The weight loss is due to the reduction of La_2CuO_4 , i.e.



The nanofibers start to be reduced at the temperature of ca. 230 °C, whereas the bulk powder begins reduction at ca. 500 °C. For the nanofiber catalyst, about 2.2 wt% weight loss is observed, while for the bulk one, the weight loss is about 0.9%. These results indicate that the one-dimensional nanofibers of La_2CuO_4 are much easier to be reduced than the bulk powder counterpart. The diameter of fibers in Fig. 1C is around 30 nm. The La_2CuO_4 lattice parameters are $a = b = 0.53 \text{ nm}$, $c = 1.30 \text{ nm}$ [27]. So we imagine that in the cross-section of the cubic fiber there are

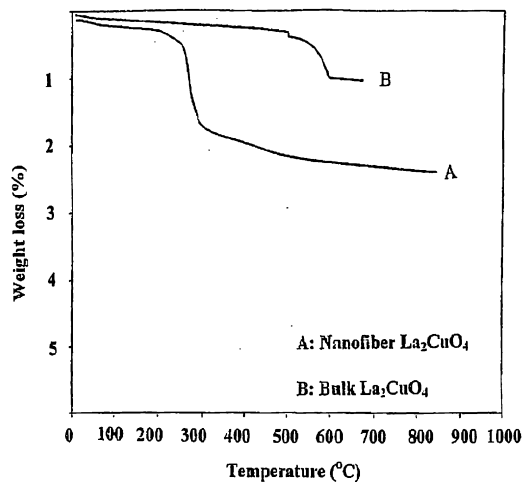


Fig. 3. Thermogravimetric (TG) curves of (A) nanofiber La_2CuO_4 and (B) bulk powder La_2CuO_4 in a H_2 flow.

about 100 La_2CuO_4 molecule units. Such 1D nanofibers are easier to be reduced than the bulk oxides. It is reasonable as in the 1D La_2CuO_4 sample there are more copper ions (may be Cu^+) with lower valence (lower oxygen coordinated) than those in the bulk powder La_2CuO_4 . The composition listed in Table 1 demonstrates that in the nanofibers there are Cu^{2+} and Cu^+ , while in the bulk powder there are Cu^{3+} and Cu^{2+} . An agreement has already been established for the methanol synthesis from syngas and its reverse reaction—SRM over cupric oxides catalysts: (i) Cu^+/Cu^0 (most likely Cu^0) are the key catalytic active sites and (ii) the highly dispersed Cu^+/Cu^0 is beneficial to the catalytic reaction. There is an optimum balance between metallic Cu^0 and oxidized Cu^+ for maximum activity/selectivity and this is a function of not only the catalyst preparation and composition but also the feed and reaction conditions [23]. The La_2CuO_4 nanofiber fulfills these two requirements. It is easier to be reduced or, in other words, the reduction of $\text{Cu}^{2+}/\text{Cu}^+$ in La_2CuO_4 nanofibers can happen at a lower temperature than that of $\text{Cu}^{3+}/\text{Cu}^{2+}$ in La_2CuO_4 bulk powder. After reduction, the copper ions and metal copper can be highly dispersed on the large nanofiber surface. The N_2O titration results listed in Table 1 indicate that the metal copper area and dispersion in the H_2 -reduced La_2CuO_4 nanofiber are both higher than those in the H_2 -reduced La_2CuO_4 bulk powder.

The EPR spectra of the H_2 -reduced bulk powder and nanofiber La_2CuO_4 samples as depicted in Fig. 4 exhibit a strong anisotropic signal with extremes at $g = 2.232$, 2.130 and 2.053; these are typical features of Cu^{2+} species; the line broadening may be from life time (spin–orbital interactions) and spin–spin dipole interactions. These results indicate that after reduction, there is still certain amount of Cu^{2+} ions in both the bulk powder and nanofiber La_2CuO_4 samples. The intensity of Cu^{2+} signal in the reduced nanofiber La_2CuO_4 is weaker than that in the bulk powder La_2CuO_4 sample, indicating that nanofibers have been deeper reduced than the bulk powder. A signal at $g = 2.007$ appears in the reduced sample of nanofiber La_2CuO_4 ; this signal can be attributed to e trapped in the oxygen vacancies [28]. The mechanism for the generation of trapped electrons could be

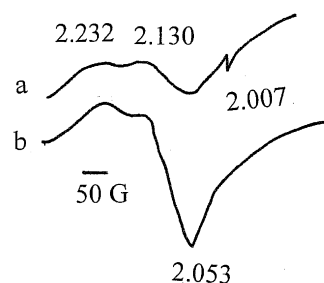
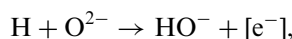
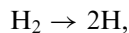


Fig. 4. EPR spectra of H_2 -reduced La_2CuO_4 (a) nanofibers and (b) bulk powder.

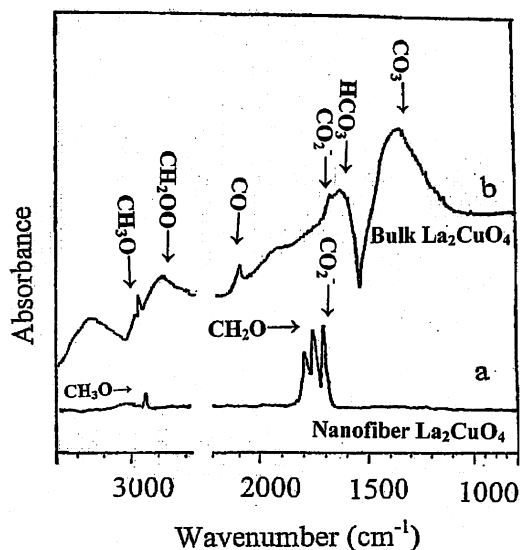


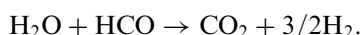
Fig. 5. *In situ* FTIR (DRIFT) spectra of methanol adsorption over the H₂-reduced La₂CuO₄ (a) nanofibers and (b) bulk powder.

Table 3
Assignments of FTIR absorbance bands

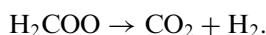
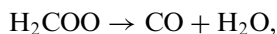
Samples	Wavenumber (cm ⁻¹)	Assignment
Nanofibers	2950	CH ₃ O _(a) (methoxide) [29,30]
	1771, 1730	CH ₂ O _(a) (formaldehyde), HCO _(a) (formyl) [30]
	1695	CO ₂ ⁻ (antisymmetric stretch) [31]
Bulk powder	2956	CH ₃ O _(a) (methoxide) [29,30]
	2870	<i>b</i> -CH ₂ OO _(a) (bidentate methylenebisoxo) [32]
	2085	CO _(a) -Cu (linear adsorbed CO on Cu ^o) [33]
	1695	CO ₂ ⁻ (antisymmetric stretch) [31]
	1600	H ₂ O _(a) , <i>b</i> -HCO ₃ _(a) (bidentate bicarbonate) [34]
	1372	<i>m</i> -CO _{3(a)} (monodentate carbonate) [35]

wherein [e⁻] represents a trapped electron located at an oxygen vacancy. Cu²⁺ can be reduced to Cu⁺ or Cu^o by picking up a trapped electron. This small signal may also be caused by the carbon impurities in the nanofibers. On the La₂CuO₄ bulk powder sample, no such trapped electrons have been generated. Fig. 5 shows the *in situ* FTIR (DRIFT) spectra of methanol adsorption over the bulk powder and nanofiber La₂CuO₄ catalysts. Table 3 lists the *in situ* FTIR (DRIFT) spectra adsorption bands and their assignments [29–35]. Over the nanofiber La₂CuO₄, the bands attributable to CH₃O (2950 cm⁻¹), HCO/H₂CO (1771, 1730 cm⁻¹) and CO₂⁻ (1695 cm⁻¹) are observed. Over the bulk powder La₂CuO₄ sample, the bands attributable to CH₃O (2956 cm⁻¹), CH₂OO (2870 cm⁻¹), CO (2085 cm⁻¹), CO₂⁻ (1695 cm⁻¹), H₂O/HCO₃ (1600 cm⁻¹) and CO₃ (1372 cm⁻¹)

are detected. CO₂⁻ was generated in both the La₂CuO₄ nanofibers sample and the La₂CuO₄ bulk powder sample. The CO species are only detected over the bulk powder La₂CuO₄ sample. The HCO/H₂CO is only detected in the nanofiber sample. Without the H₂O steam, the decomposition of HCOO/H₂COO could produce CO₂ and H₂. HCO/H₂CO may react with the lattice oxygen or other surface oxygen species such as hydroxyl in the catalyst to produce CO₂. As it is difficult to carry out the *in situ* FTIR experiment of water steam adsorption, we perform the methanol/H₂O pulse reaction over the nanofiber and bulk powder samples at 300 °C, respectively. After adsorption of methanol, water steam is pulsed. Over the nanofiber catalyst, only CO₂ is generated. Over the bulk powder sample, CO and CO₂ are co-produced. We deduce that over the nanofibers



Normally the HCO or H₂CO is rapidly decarbonylated to CO and H₂, and then partially transformed to CO₂ and H₂ through the secondary WGS reaction [36,37]. Over nanofiber, we cannot observe the adsorbed CO vibration band, but we find HCO/H₂CO. The oxygen vacancy with the trapped electron in the nanofiber catalyst may stabilize the HCO and H₂CO and prevent them from decomposing to CO and H₂ directly. In the spectrum of methanol adsorption over the La₂CuO₄ bulk powder, we cannot detect the H₂CO/HCO species, but we find the CH₂OO and adsorbed CO species. We assume that two possibilities may occur: firstly, the H₂CO/HCO is extremely unstable and has already decomposed to CO and H₂; secondly, the CH₂OO species may go through the two decomposition ways:



In the FTIR spectrum, the adsorbed H₂O is detected.

4. Conclusion

- The La₂CuO₄ nanofiber is prepared by using CNTs as templates. Compared with the La₂CuO₄ bulk powder sample, the nanofiber is of higher specific surface area. The La₂CuO₄ bulk powder is composed of Cu³⁺, Cu²⁺ and extra-oxygen species while the La₂CuO₄ nanofiber is composed of Cu²⁺, Cu⁺ and oxygen vacancies. The nanofiber can be reduced at lower temperature and to a farther extent than the bulk powder counterpart. After being reduced, the Cu-metal area and Cu^o dispersion in the nanofibers are higher than those in the bulk powder.
- For the reaction of SRM to produce CO₂ and hydrogen, the La₂CuO₄ nanofiber shows a much better

catalytic performance in terms of methanol conversion, CO₂ selectivity and catalyst lifespan. When the temperature is 150 °C, 100% methanol is converted (13.8 g/h g catalyst). At temperatures below 300 °C, the products are only H₂ and CO₂ without CO. Over the nanofiber catalyst, the oxygen vacancy together with the trapped electron may stabilize the intermediates of HCO and H₂CO and prevent them from decomposing to CO and H₂. Over the bulk catalyst, the intermediate H₂COO may decompose to CO and H₂O.

References

- [1] Editorial, *Nature* 427(6976) (2004) 661.
- [2] M.Z. Jacobson, W.G. Colella, D. Golden, *Science* 308 (24) (2005) 1901.
- [3] W. Grochala, P.P. Edwards, *Chem. Rev.* 104 (2004) 1283.
- [4] P. Chen, Z. Xiong, J. Luo, J. Lin, K.L. Tan, *Nature* 420 (2002) 302.
- [5] B.C.H. Steele, A. Heinzl, *Nature* 414 (2001) 345.
- [6] M. Schroepe, *Nature* 414 (2001) 682.
- [7] T. Shishido, Y. Yamamoto, H. Morioka, K. Takaki, K. Takehira, *Appl. Catal. A* 263 (2004) 249.
- [8] B.A. Peppley, J.C. Amphett, L.N. Kearns, R.F. Mam, *Appl. Catal. A* 179 (1999) 31.
- [9] J. Bravo, A. Karim, T. Conant, G.P. Lopez, A. Datye, *Chem. Eng. J.* 101 (2004) 113.
- [10] S. Fukahori, T. Kitaoka, A. Tomoda, R. Suzuki, H. Wariishi, *Appl. Catal. A* 300 (2006) 155.
- [11] I. Ritzkopf, S. Vukojević, C. Weidenthaler, J.D. Grunwaldt, F. Schüth, *Appl. Catal. A* 302 (2006) 215.
- [12] T. Tanabe, S. Kameoka, A.P. Tsai, *Catal. Today* 111 (2006) 153.
- [13] C.Z. Yao, L.C. Wang, Y.M. Liu, G.S. Wu, Y. Cao, W.L. Dai, H.Y. He, K.N. Fan, *Appl. Catal. A* 297 (2006) 151.
- [14] L.Z. Gao, C.T. Au, *J. Catal.* 189 (2000) 1.
- [15] L.Z. Gao, X.L. Wang, H.T. Chua, S. Kawi, *J. Solid State Chem.* 179 (2006) 2044.
- [16] D.C. Harris, T.A. Hewston, *J. Solid State Chem.* 69 (1987) 182.
- [17] L.Z. Gao, C.T. Au, *J. Mol. Catal. A* 168 (2001) 173.
- [18] J.T. Li, W.D. Zhang, L.Z. Gao, P.Y. Gu, K.Q. Sha, H.L. Wan, *Appl. Catal. A* 165 (1997) 411.
- [19] B.C. Liu, L.Z. Gao, Q. Liang, S.H. Tang, M.Z. Qu, Z.L. Yu, *Catal. Lett.* 71 (2001) 225.
- [20] H. Li, Q. Li, L.Z. Gao, C.T. Au, Z.L. Yu, *Catal. Lett.* 74 (2001) 185.
- [21] N. Guilhaume, S.D. Peter, M. Primet, *Appl. Catal. B* 10 (1996) 325.
- [22] D.R. Palo, J.D. Holladay, R.A. Dagle, Y.-H. Chin, *ACS Symp. Ser.* (2005) 209.
- [23] D.R. Palo, R.A. Dagle, J.D. Holladay, *Chem. Rev.* 107 (2007) 3992.
- [24] L.W. Pan, S.D. Wang, *Int. J. Hydrogen Energy* 30 (2005) 973.
- [25] M. Twigg, M. Spencer, *Top. Catal.* 22 (2003) 192.
- [26] R.D. Cortright, R.R. Davda, J.A. Dumesic, *Nature* 418 (2002) 964.
- [27] M.J. Akhtar, C.R.A. Catlow, S.M. Clark, W.M. Temmerman, *J. Phys. C* 21 (1988) L917.
- [28] L.Z. Gao, C.T. Au, *Appl. Catal. B* 30 (2001) 35.
- [29] G.J. Millar, C.H. Rochester, K.C. Waugh, *J. Chem. Soc. Faraday Trans.* 88 (1992) 1033.
- [30] I.A. Fisher, A.T. Bell, *J. Catal.* 172 (1997) 222.
- [31] G.J. Millar, C.H. Rochester, *Top. Catal.* 3 (1996) 103.
- [32] E.M. Stuve, R.J. Madix, B.A. Sexton, *Surf. Sci.* 119 (1982) 279.
- [33] D.B. Clarke, D.K. Lee, M.J. Sandoval, A.T. Bell, *J. Catal.* 142 (1993) 27.
- [34] W. Hertl, *Langmuir* 5 (1989) 96.
- [35] J.F. Edwards, J.L. Schrader, *J. Phys. Chem.* 88 (1984) 5620.
- [36] N. Takezawa, N. Iwasa, *Catal. Today* 36 (1997) 45.
- [37] N. Iwasa, T. Mayanagi, N. Wataru, M. Arai, T. Takewasa, *Appl. Catal. A* 248 (2003) 153.